RSC Advances

[Fe(bipy)Cl4][bipy.H] hosted by Al-MCM-41: an efficient Dibenzo[b,f][1,4]oxazepine (CR) decontamination nano-reactor

Journal:	*RSC Advances*
Manuscript ID:	RA-ART-03-2015-004565.R1
Article Type:	Paper
Date Submitted by the Author:	27-Mar-2015
Complete List of Authors:	Khorshidi, Alireza; University of Guilan, chemistry Heidari, Sirous; University of Guilan,

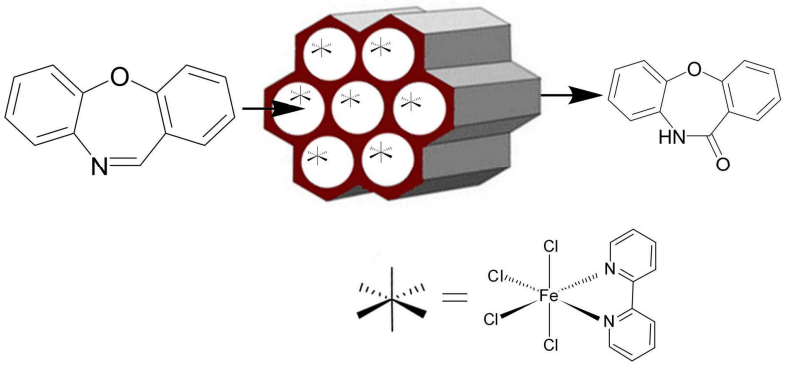

[Fe(bipy)Cl_4][bipy.H] hosted by Al-MCM-41: an efficient Dibenzo[*b*,*f*][1,4]oxazepine (CR) decontamination nano-reactor

[Fe(bipy)Cl_4][bipy.H] hosted by Al-MCM-41: an efficient Dibenzo[*b,f*][1,4]oxazepine (CR) decontamination nano-reactor

Alireza Khorshidi[1*], Sirous Heidari[1]

[1] Department of Chemistry, Faculty of Sciences, University of Guilan, P. O. Box: 41335-1914, Iran

** Corresponding author's email: Khorshidi@guilan.ac.ir*

Abstract: Encapsulation of [Fe(bipy)Cl_4][bipy.H] (**1**) (where bipy is 2,2′-bipyridine) in the Al-MCM-41 molecular sieve by using a "ship in a bottle synthesis" approach was achieved and the product characterized by X-ray diffraction, FTIR, DRS, TG, EDS and BET analysis. Encapsulation of the complex into the channels of Al-MCM-41, did not affect morphology of the host as it is evident from SEM and TEM micrographs. The obtained nanocatalyst in combination with $K_2S_2O_8$ as the oxidant, was successfully used in selective catalytic conversion of dibenzo[*b,f*][1,4]oxazepine (CR, riot control agent) to dibenzo[*b,f*][1,4]oxazepin-11(10*H*)-one as a potential decontamination route. Good selectivity was also obtained toward formation of benzil in the oxidation of *trans*-stilben.

Keywords: [Fe(bipy)Cl_4][bipy.H]; Encapsulation; Mesoporous; Al-MCM-41; Dibenzo[*b,f*][1,4]oxazepine; Decontamination

1. Introduction

Encapsulation of transition metal complexes inside inorganic structures makes it possible to design catalysts which combine the advantages of homogeneous and heterogeneous catalytic systems [1]. Molecular sieves are attractive hosts, as they combine high thermal and chemical stability with a quite regular crystalline framework structure. The well-defined and ordered structure of them provides an ideal environment to entrap active metal complexes, and the confinement leads to higher stability by reducing dimerization of active sites. These modified systems can be exploited as catalysts. Both zeolites and mesoporous material such as MCM-41 have been used for this purpose. For example, Balkus et al reported zeolite encapsulated metal complexes [2], Xavier et al, prepared intrazeolite cobalt(II), nickel(II) and copper(II) complexes of 3-formylsalicylic acid for

oxidation reactions [3] and Yamaguchi et al, recently reported selective hydroxylation of cyclohexene over Fe-bipyridine complexes encapsulated into zeolite Y under environment-friendly conditions [4]. In addition to zeolites, mesoporous structures such as MCM-41 also, have been studied. Some reports in this context include trimethylstannyl molybdenum complex hosted by MCM-41 [5], Fe(III)-salen encapsulated Al-MCM-41 as a catalyst in polymerization of bisphenol-A [6], metallo octamethylcalix pyridine complexes encapsulated in MCM-41 [7], Zn(II) phthalocyanines immobilized in mesoporous silica Al-MCM-41 for photocatalytic degradation of pesticides [8] and dinuclear iron 1,10-phenanthroline complex encapsulated in MCM-41 for oxidation of benzyl alcohol [9].

Due to the steric constraint of these hosts, however, interesting changes in the physicochemical properties of such encapsulated complexes have been reported [10–13].

Mixed ligand complexes, on the other hand, can be a synthetic challenge to tune properties of transition metal complexes. Metal complexes containing diimine ligands such as 1,10-phenanthroline and bipyridine have attracted attention because of their versatile roles as building blocks for the synthesis of metallodendrimers and as molecular scaffolding for supramolecular assemblies, and in analytical chemistry, catalysis, electrochemistry, ring-opening metathesis polymerization (ROMP) and biochemistry. However, most diimine complexes reported so far, are homo ligand compounds of the general formula $M(N–N)_3$ or to a lesser extent $M(N–N)_2X_2$. To the best of our knowledge, little attention has been paid to the incorporation of hetero ligand complexes into the molecular sieves. Dibenzo[*b,f*][1,4]oxazepine (CR), on the other hand, is an incapacitating and a lachrymatory agent. CR was first synthesized in 1962 [14] and is a pale yellow crystalline solid with a pepper-like odor. It is chemically stable and does not degrade with time. The dibenzo[*b,f*][1,4]oxazepine moiety is present in the typical antipsychotic drug loxapine (Figure 1), but, unlike CR, loxapine is not reactive and is not an irritant.

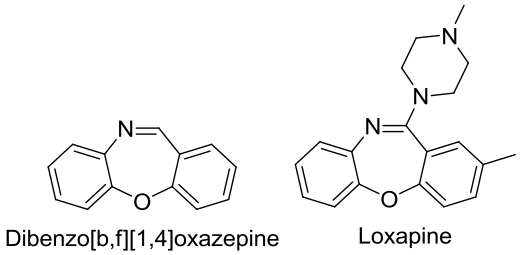

Figure 1. dibenzo[*b,f*][1,4]oxazepine and loxapine

Our interest in the study of ion-exchanged zeolites and encapsulated species [15, 16], prompted us to evaluate [Fe(bipy)Cl_4][bipy.H] encapsulated in molecular sieves as a selective oxidation catalyst and the results were satisfying.

2. Experimental

2.1 Reagents and materials

All materials were purchased from Merck and used without further purification. [Fe(bipy)Cl_4][bipy.H] was synthesized according to Safari et al [17]. In brief, 2,2′-bipyridine (0.155g, 1 mmol) was dissolved in 0.1 M HCl (10 ml). $FeCl_3.6H_2O$ (0.135 g, 0.5 mmol) in water (10 ml) was added to this solution, and the resulting red solution was stirred at 55–60 ^oC for 3h. The product was obtained from CH_3CN as orange prismatic crystals after 3 days. (Yield: 0.195 g, 76.3%). m.p.: 216 ^oC, IR (KBr, cm^{-1}): 3060, 1615, 1599, 1583, 1443, 1311, 1270, 1248, 1229, 1174, 1158, 1021, 764, 733, 652, 630, 357, 333, 309 (Fe–Cl), 291 (Fe–Cl), 258 (Fe–N).

Al-MCM-41 with a Si/Al ratio of 39 was synthesized and characterized according to the literature [18]. The Fe^{3+} ion-exchanged molecular sieve was obtained by overnight stirring of the Al-MCM-41 with 0.05 M solution of $FeCl_3.6H_2O$ (15 mL per g of Al-MCM-41), then filtration and washing with hot deionized water to remove any physisorbed species, as was monitored by a conductometer. The whole process repeated three times and soxhlet extraction with acetonitrile removed the ions located on the host's surface. Finally, the ion-exchanged material was subsequently filtered and calcined at 550 ^oC.

In order to encapsulate [Fe(bipy)Cl_4][bipy.H] in the host, 2,2′-bipyridine (0.155g, 1 mmol, excess) was dissolved in 10 mL of a 1:1 mixture of ethanol and water and titrated

by 0.1 M HCl to pH of 7.0. To this solution, 500 mg of the corresponding ion-exchanged host was added and the mixture was stirred at 55–60 ^{o}C for 3h. The orange product was then filtered and washed with hot deionized water three times, then soxhlet extracted with acetonitrile. The iron content of the catalyst (Al-MCM-41-[Fe(bipy)Cl_4][bipy.H]) was determined by using inductively coupled plasma (ICP) as 1.848%.

2.2 General procedure for the oxidation reactions:

Caution: dibenzo[*b,f*][1,4]oxazepine is highly irritating.

Dibenzo[*b,f*][1,4]oxazepine (1.0 mmol) was dissolved in 5.0 mL of ethanol and potassium persulfate (0.5 mmol in 5.0 mL of dimethylformamide) was added to the solution. Then 20 mg of the catalyst was added and the mixture stirred at 50 ^{o}C under reflux condition. Progress of the reaction was monitored by TLC (*n*-hexane/ethyl acetate: 10/4). After 1h, the reaction mixture was filtered and quenched with 10 mL of cold water. The gray precipitate was filtered and recrystallized from ethyl acetate to provide pure dibenzo[*b,f*][1,4]oxazepin-11(10*H*)-one.

Dibenzo[*b,f*][1,4]oxazepin-11(10*H*)-one:

Gray solid, M.P. 208-211 ^{o}C, FTIR (KBr, υ/cm^{-1}): 3062, 2931, 1676, 1607, 1448, 1204 and 767. ^{1}H NMR (400 MHz, DMSO-d_6): δ 11.21 (s, 1H), 8.03 (d, 1H, *J*= 7.6 Hz), 7.85 (br, 2H), 7.53 (t, 1H, *J*= 7.6 Hz), 7.48-7.44 (m, 2H), 7.14 (d, 2H, *J*= 8.4 Hz), 7.09 (t, 1H, *J*= 7.6 Hz) ppm. ^{13}C NMR (100 MHz, DMSO-d_6): δ 162.8, 158.2, 149.3, 139.9, 134.4, 128.1, 126.3, 125.8, 120.4, 119.7, 117.6, 111.5, 110.9 ppm.

Trans-stilbene (1.0 mmol) and KIO_4 (0.5 mmol) were added to 10 mL of a mixture of acetonitrile and dimethylformamide (1:9), and then 30 mg of the catalyst was added. The reaction mixture was stirred at 60 ^{o}C under reflux condition. Progress of the reaction was monitored by TLC (*n*-hexane/ethyl acetate: 10/2). After 1h, the reaction mixture was filtered and the products were purified by using preparative TLC (*n*-hexane/ethyl acetate: 10/2), and characterized from their FTIR spectra in comparison with authentic samples.

2.3 **Instrumentation**

X-ray powder diffraction (XRD) measurements were performed by using a Philips diffractometer of X'pert Company with mono chromatized Cu k_α radiation. IR spectra were recorded on a Shimadzu FTIR-8400S spectrometer. Morphology of the synthesized samples was characterized with a scanning electron microscope (SEM) from Philips

Company (XL30 ESEM). TEM images were obtained on a transmission electron microscope (TEM-PHILIPS MC 10) with an acceleration voltage of 80 kV. ^{1}H NMR spectra were obtained on a Bruker DRX-400 Avance spectrometer and ^{13}C NMR spectra were obtained on a Bruker DRX-100 Avance spectrometer. Chemical shifts of ^{1}H and ^{13}C NMR spectra were expressed in ppm downfield from tetramethylsilane. Melting points were measured on a Büchi Melting Point B-540 instrument and are uncorrected.

3. Results and discussion

Treatment of one equivalent of $FeCl_3.6H_2O$ with 2 equivalents of the bidentate chelating ligand, bipy, in the presence of HCl solution affords a compound with the formula $[Fe(bipy)Cl_4][bipy.H]$. The structure of complex **1** is unambiguously identified [19]. Considering our interest in the transition metal catalytic systems and difficulty of recovering homogeneous transition metal complexes, we decided to encapsulate complex **1** in mesoporous Al-MCM-41, as a potential heterogeneous alternative. The unit cell parameters of the complex **1** (a= 15.938(2) Å, b= 9.3068(15) Å, c=14.513(3) Å, z=4, R_1=0.0406, Figure 2) [19], are proportional to the Al-MCM-41 pore size.

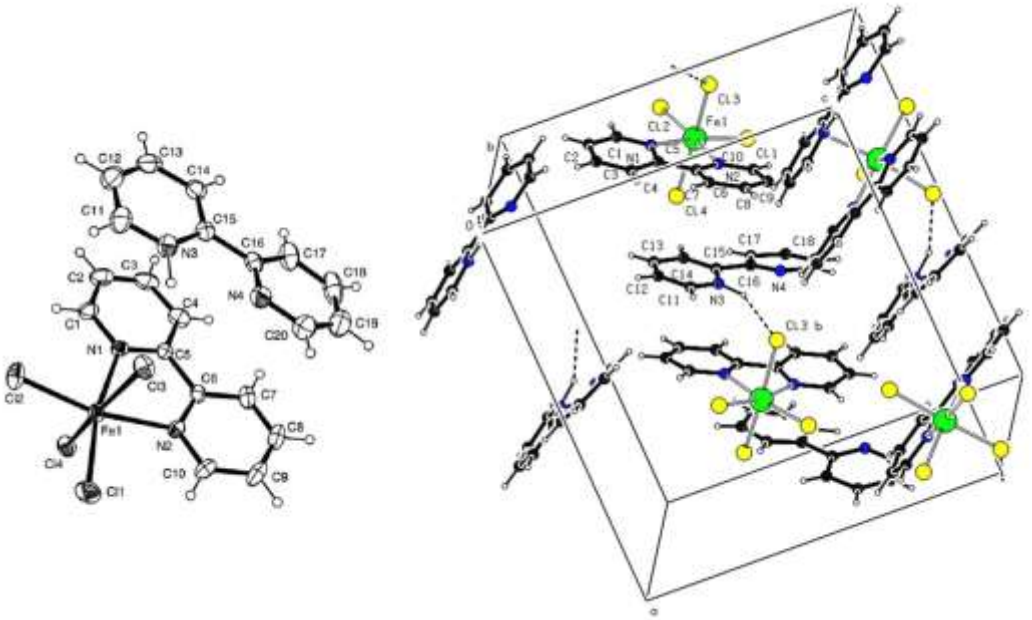

Figure 2. The labeled diagram of $[Fe(bipy)Cl_4][bipy.H]$ (left), and its unit cell structure with hydrogen bonds shown as dashed lines (right) [19].

To do so, a "ship in a bottle synthesis" approach was selected. Fe^{3+} loaded Al-MCM-41 (Fe^{III}-Al-MCM-41) is yellow in color. Upon diffusion of the 2,2′-bipyridine ligand into the channels of Al-MCM-41, however the color changed to red, which is the first characteristic of formation of the desired complex. Feasibility of the synthesis however, was approved by FT-IR spectra and XRD patterns. Figure 3a shows the FT-IR spectra of **1**, and Figure 3b shows FT-IR spectra of the Al-MCM-41 loaded $[Fe(bipy)Cl_4][bipy.H]$. No peaks associated to stretching vibrations mode of Fe-O in the region of 580-640 cm^{-1} were observed, which diminished the formation of iron(III) oxide during calcination.

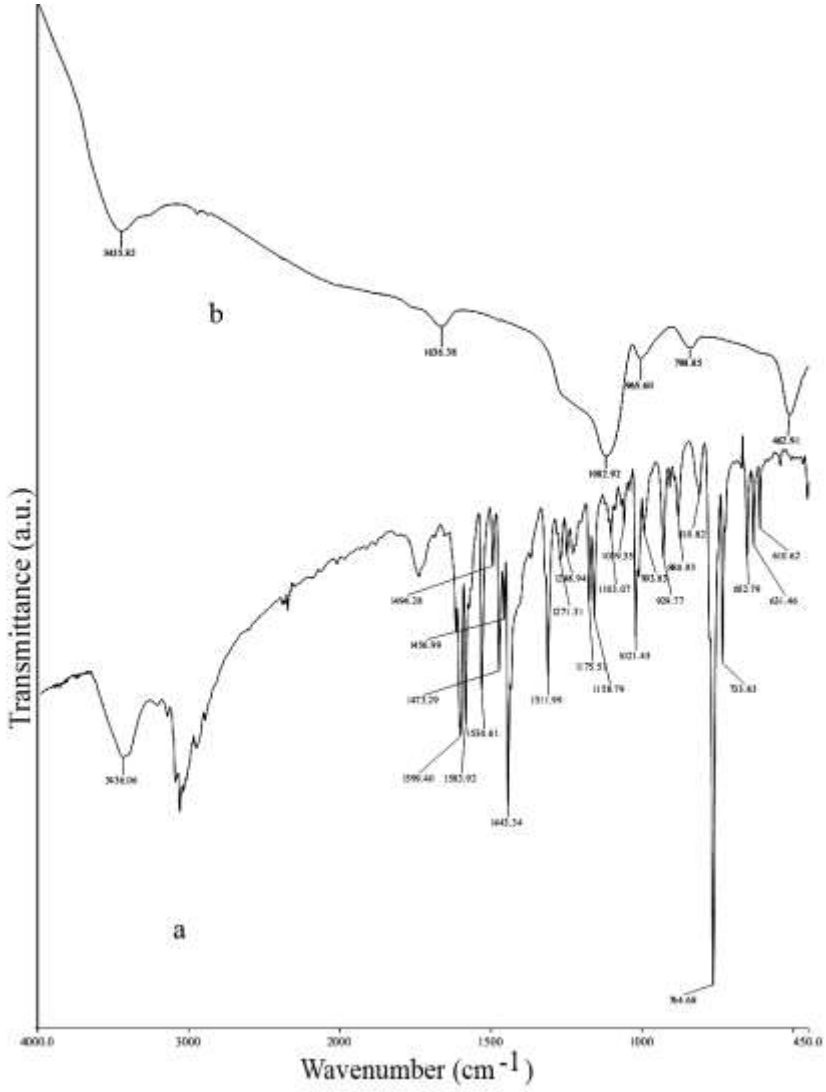

Figure 3. FT-IR spectrum of $[Fe(bipy)Cl_4][bipy.H]$ (a) and Al-MCM-41 loaded $[Fe(bipy)Cl_4][bipy.H]$ (b)

While little could be deduced from these spectra, which is due to broad and strong absorption bands of the host, IR spectroscopy in the region of 200-400 cm^{-1} provided more useful details. As it is obvious from Figure 4a, complex **1** shows three characteristic bands at 309 (Fe–Cl), 291 (Fe–Cl) and 258 (Fe–N) cm^{-1} [17]. The same vibrations were observed for Al-MCM-41 loaded $[Fe(bipy)Cl_4][bipy.H]$ (Figure 4b).

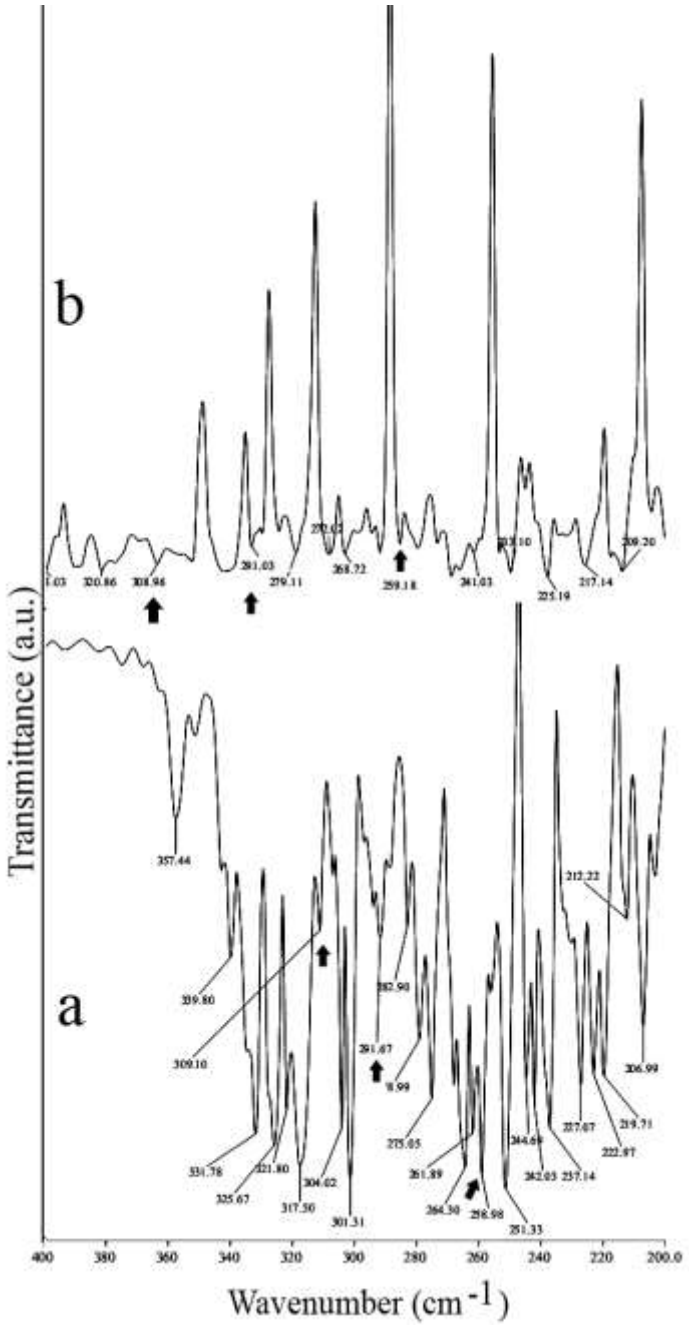

Figure 4. FT-IR spectrum of complex **1** (a) and Al-MCM-41 loaded complex **1** (b) in the region of 200-400 cm^{-1}

XRD patterns of free and Al-MCM-41-encapsulated complex **1**, also confirm feasibility of the synthesis (Figure 5). Four index peaks of the complex **1** (Figure 5a) at 2θ=12, 25.5, 26 and 29.2^{o} reoccurred in the XRD pattern of the encapsulated complex (Figure 5b). Inset of the Figure 5b, also, shows low angle pattern for the Al-MCM-41-encapsulated complex **1,** indicating that the crystal structure of Al-MCM-41 was retained after incorporation [20].

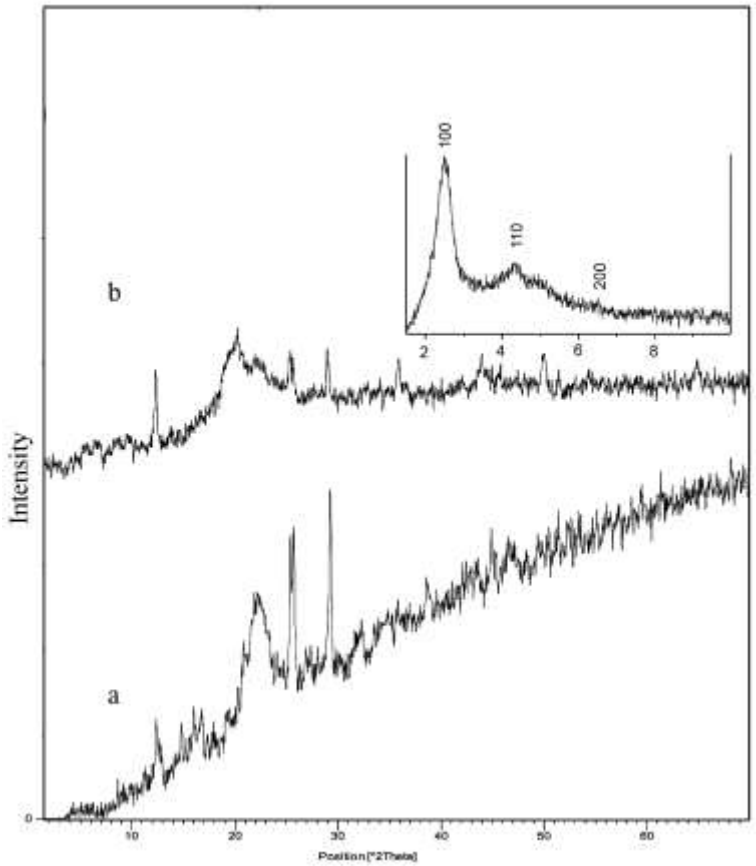

Figure 5. XRD patterns of [Fe(bipy)Cl_4][bipy.H] (a) and Al-MCM-41-encapsulated [Fe(bipy)Cl_4][bipy.H] (b). Inset shows low angle pattern for the Al-MCM-41-encapsulated complex [Fe(bipy)Cl_4][bipy.H]

Incorporation of the complex **1** into the channels of Al-MCM-41 did not affect morphology of the host as it is evident from SEM micrographs. As shown in Figure 6, the Al-MCM-41 crystallites of about 1 μm, preserved their size and shape after hosting the complex, and a close-up image also showed that the structure of channels were preserved, too. TEM image taken with the electron beam parallel to the pore direction showed a

highly ordered hexagonal structure with slight occlusion (Figure 6d). In the other images there was no evidence of the formation of complex nanoparticles outside the pores. EDS analysis of the composite (Figure 6f), on the other hand, confirmed the presence of complex **1**, probably with a uniform distribution inside the channels rather than formation of aggregates or nanocrystals.

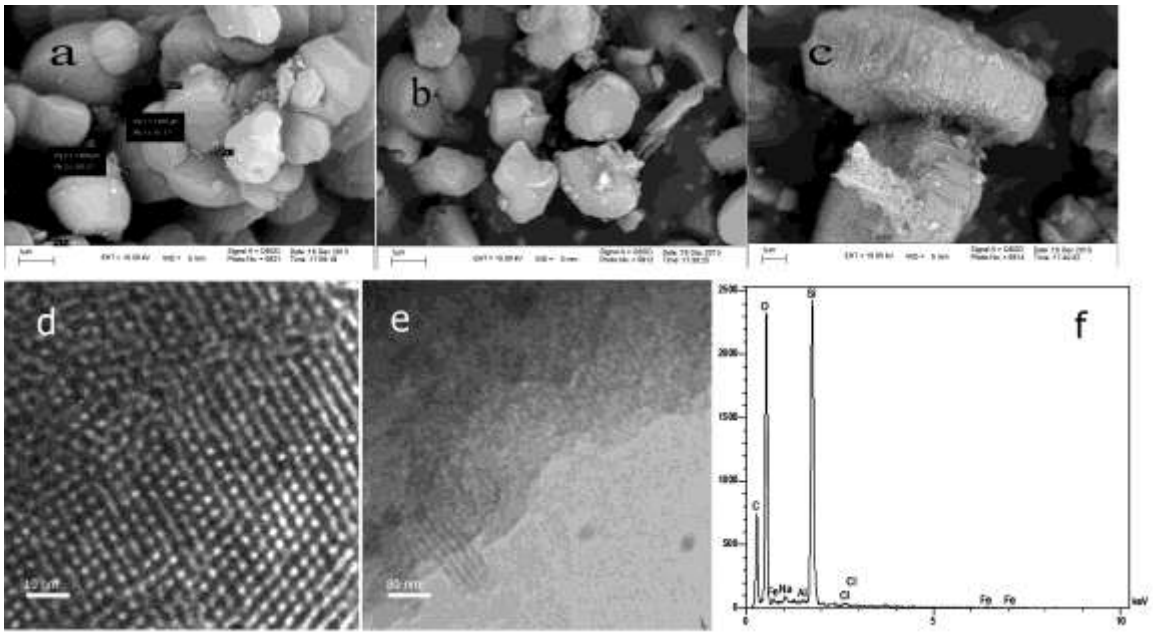

Figure 6. SEM images of Al-MCM-41 (a) and Al-MCM-41 loaded [Fe(bipy)Cl_4][bipy.H] (b, c), TEM image of Al-MCM-41 loaded [Fe(bipy)Cl_4][bipy.H] (d, e), EDS analysis of Al-MCM-41 loaded [Fe(bipy)Cl_4][bipy.H]

The N_2 adsorption-desorption isotherms of calcined Al-MCM-41 and Al-MCM-41 loaded [Fe(bipy)Cl_4][bipy.H] exhibit type IV behavior, typical for mesoporous materials with two dimensional hexagonal structure (Figure 7). As it is obvious from Figure 7b, in the case of Al-MCM-41 loaded [Fe(bipy)Cl_4][bipy.H] the amount of adsorbed nitrogen decreases and the small hysteresis loop observed at relative pressures about 0.3 for Al-MCM-41 shifts to lower values. The decrease in the absorption amount may be attributed to the reduced surface area, and shift of the inflection point may be resulted from pore filling effect due to incorporation of the complex into the mesoporous structure. BET surface area of Al-MCM-41 dropped from 930.0 m^2/g to 703.9 m^2/g for impregnated host. Drop in pore volume was from 0.88 mL/g to 0.69 mL/g, and as expected, BJH maxima of the pore size distribution decreased from 3.8 to 2.6 nm.

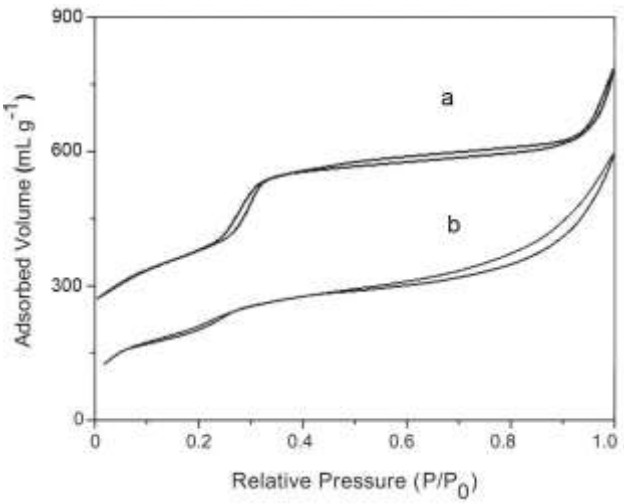

Figure 7. N_2 adsorption-desorption isotherms of Al-MCM-41 (a) and Al-MCM-41 loaded $[Fe(bipy)Cl_4][bipy.H]$ (b)

Thermogravimetric (TG) analysis of the as-synthesized product (Figure 8a) consists of distinct parts: a) Loss of physisorbed water from 80 to 180 ^oC, which corresponds to the water molecules absorbed on the external surface and those hosted in the pores, b) collapsing of the complex molecules from 215 to 250 ^oC and c) condensation of silanol groups from 350 to 600 ^oC. It could be deduced that the obtained catalyst has enough thermal stability to endure recycling processes or harsh reaction conditions up to 200 ^oC. The TG curve of the $[Fe(bipy)Cl_4][bipy.H]$ complex is also shown for comparison in Figure 8b.

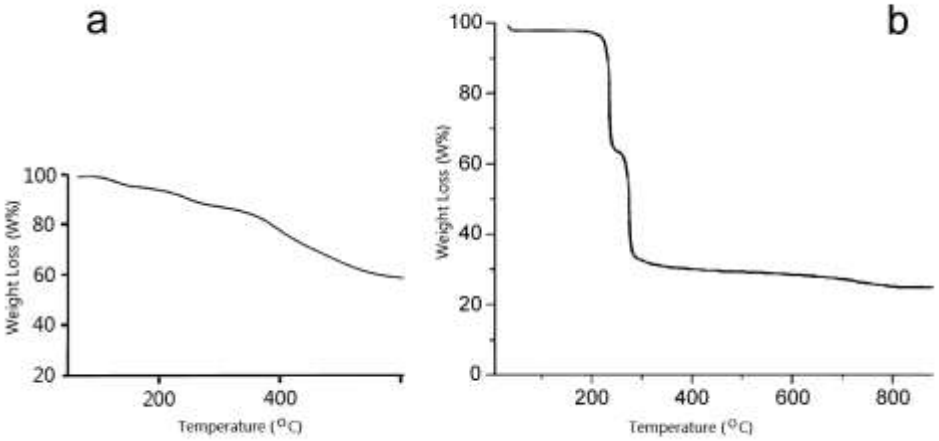

Figure 8. TG curve for the Al-MCM-41-encapsulated [Fe(bipy)Cl_4][bipy.H] (a), and [Fe(bipy)Cl_4][bipy.H] complex (b)

To further confirm the presence of complex inside the channels of mesoporous material, the diffuse reflectance spectra were obtained. As shown in figure 9, the Al-MCM-41 shows no absorbance in the visible range (Figure 9a). [Fe(bipy)Cl_4][bipy.H] complex on the other hand, exhibited a broad absorption in the range of 450-500 nm (Figure 9b), corresponding to transitions from $^1A_1 \rightarrow {}^1T_1$ for a d^6 configuration in a pseudo-octahedral field which results in the orange color of the complex. The same transitions were observed in the DRS spectrum of Al-MCM-41-[Fe(bipy)Cl_4][bipy.H].

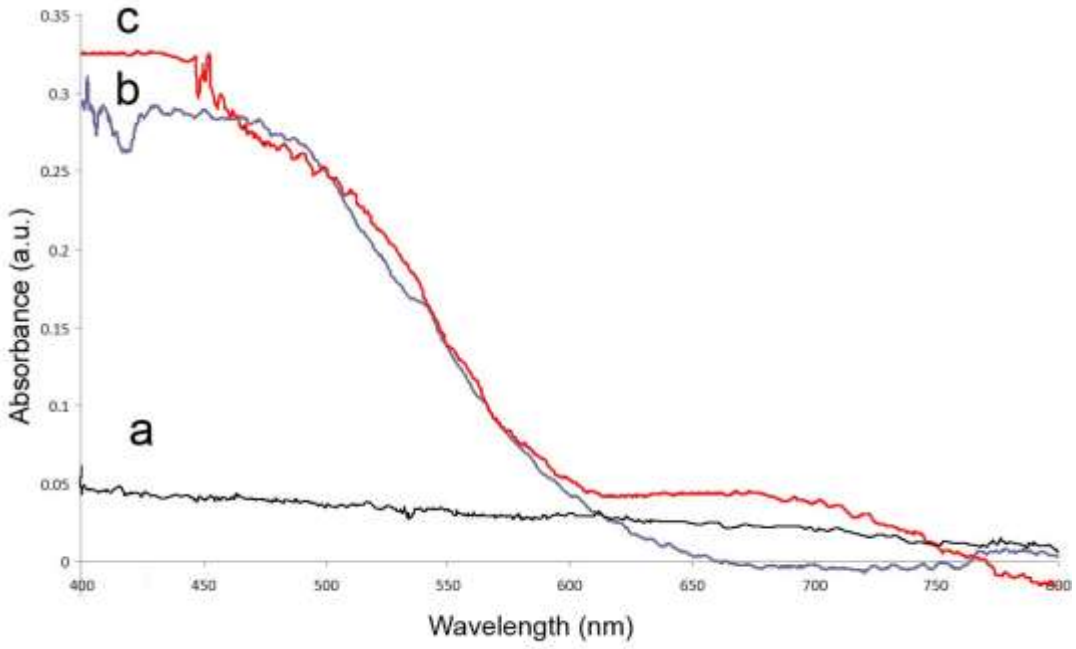

Figure 9. Diffuse reflectance spectra (DRS) of Al-MCM-41 (a), [Fe(bipy)Cl_4][bipy.H] (b) and Al-MCM-41-encapsulated [Fe(bipy)Cl_4][bipy.H] (c)

Having encapsulated complex in hand, we decided to evaluate its application in selective oxidative transformations. The chemistry of CR derivatives has attracted attention due to their importance in biologically active compounds [21, 22]

3-ring heterocyclic compounds, to which the CR belongs, have widespread application in medicine as anti-depressant agents. The CR itself, however, is chemically stable and little has been reported on its reactions such as chlorination and oxidation, thus far [23-25].

Brewster *et al* [26] reported the oxidation of CR derivatives in glacial acetic acid by using H_2O_2 overnight, which provided a mixture of lactam, phenoxazine, benzoxazole and other products. Harrison *et al*, on the other hand, reported the metabolism of CR and its *in vivo* hydroxylation which provided a mixture of lactam, 4-hydroxylactam and 7-hydroxylactam [27]. Due to application of dibenzo[*b*,*f*][1,4]oxazepin-11(*10H*)-one derivatives as intermediates in the synthesis of Loxapine and Amoxapine [28, 29], selectivity in the oxidation of CR toward lactam product would be of great interest.

In order to achieve selective transformation of the CR substrate to the lactam product, in presence of the Al-MCM-41 loaded [Fe(bipy)Cl_4][bipy.H] as a heterogeneous catalyst, first the reaction conditions were optimized with regard to the catalyst type, catalyst loading, oxidant and solvent. As shown in Table1, by using KIO_4 as the oxidant, in the absence of the catalyst, no formation of the desired product was observed and the optimum loading was 20 mg of the catalyst per mmol of the substrate (entry 3). Although under the same condition, free [Fe(bipy)Cl_4][bipy.H] resulted in excellent yield of 99%, but recycling of the catalyst was problematic. To optimize the reaction time and exclude the equilibrium of the reaction, and to clarify the performance, shorter reaction times were tested (entries 5-10). It was found that the homogeneous catalyst had superiority against the heterogeneous counterpart in terms of the reaction time. Heterogeneous catalyst, on the other hand, had the advantage of easy recycling which promises minimization of the waste. Fe(III)-ion exchanged Al-MCM-41 was also tested and a lower yield was obtained under the same condition (entry12). The Al-MCM-41 host itself, however, resulted in no desirable product. It was also found that the yield of the product was solvent dependant, and the best solvent was found to be a 1:1 mixture of ethanol and dimethylformamide. The catalytic performance of Al-MCM-41 loaded [Fe(bipy)Cl_4][bipy.H] was compared with a mixture of Al-MCM-41 and [Fe(bipy)Cl_4][bipy.H] with exactly the same metal to host ratio (1.8% w/w Fe). Although the excellent yield of 92% was obtained in 45 min (entry 14), but filtration of the reaction mixture only resulted in pure Al-MCM-41 host. This may confirm heterogeneity of our catalyst and success of encapsulation. With regard to the oxidant, $K_2S_2O_8$ was also tested and resulted in excellent yield of 98 %. The optimized conditions are summarized in Scheme 1.

Table 1. The effect of various parameters on the oxidation reaction of dibenzo[*b*,*f*][1,4]oxazepine

Entry [a]	Catalyst	Catalyst loading (mg)	Time (min)	Yield [b] (%)
1	Al-MCM-41-[Fe(bipy)Cl_4][bipy.H]	0	60	0 [c]
2	Al-MCM-41-[Fe(bipy)Cl_4][bipy.H]	10	60	84 [c]
3	Al-MCM-41-[Fe(bipy)Cl_4][bipy.H]	20	60	95 [c]
4	Al-MCM-41-[Fe(bipy)Cl_4][bipy.H]	30	60	95 [c]
5	Al-MCM-41-[Fe(bipy)Cl_4][bipy.H]	20	10	32
6	Al-MCM-41-[Fe(bipy)Cl_4][bipy.H]	20	20	45
7	Al-MCM-41-[Fe(bipy)Cl_4][bipy.H]	20	30	64
8	Al-MCM-41-[Fe(bipy)Cl_4][bipy.H]	20	45	78
9	[Fe(bipy)Cl_4][bipy.H]	10	10	68
10	[Fe(bipy)Cl_4][bipy.H]	10	30	91
11	[Fe(bipy)Cl_4][bipy.H]	10	60	99 [c]
12	Fe^{III}- Al-MCM-41	20	60	73 [c]
13	Al-MCM-41	20	60	0 [c]
14	Al-MCM-41 + [Fe(bipy)Cl_4][bipy.H]	20 [d]	60	92
15	Al-MCM-41-[Fe(bipy)Cl_4][bipy.H]	20	60	98[e]

[a] All reactions were carried out at 50 ^oC under reflux condition.

[b] Isolated yields.

[c] KIO_4 as the oxidant.

[d] 1.8% w/w Fe/Al-MCM-41

[e] $K_2S_2O_8$ as the oxidant.

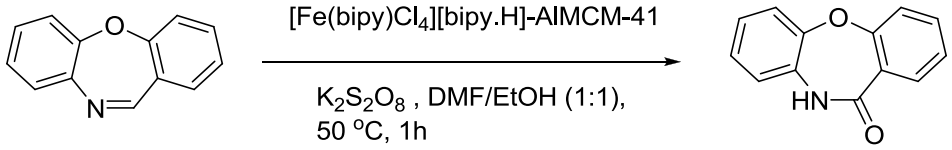

Scheme 1. Selective oxidation of dibenzo[*b*,*f*][1,4]oxazepine to dibenzo[*b*,*f*][1,4]oxazepin-11(10*H*)-one

Although the precise mechanism of the reaction awaits further studies, a proposed mechanistic pathway which rationalizes the selective product formation, is presented in Scheme 2.

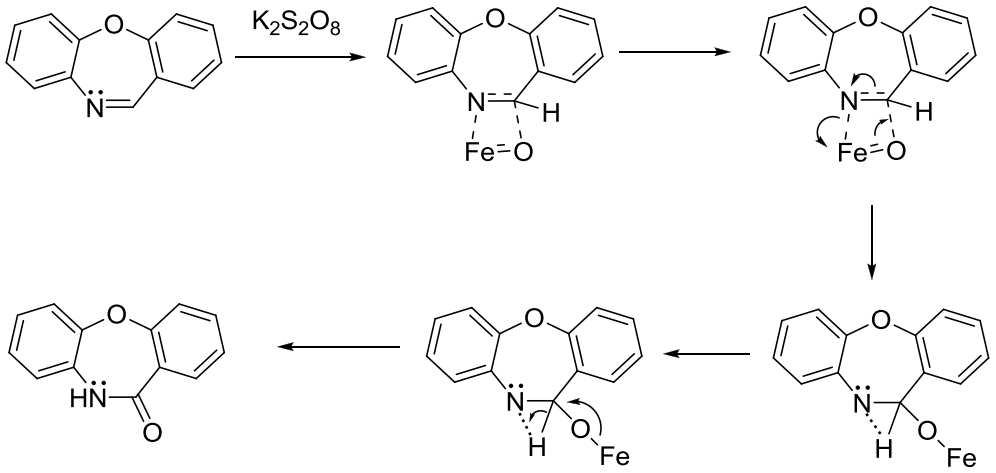

Scheme 2. Proposed mechanism for the oxidation of CR

As it is shown, a four-membered ring intermediate may be involved in the reaction, which in turn provides the lactam product upon rearrangement. Encouraged by these results, we decided to evaluate efficiency of this protocol in the oxidation of *trans*-stilbene. Generally, oxidation of *trans*-stilbene may produce a mixture of products such as epoxide, benzil, benzaldehyde and benzoic acid. Under catalysis of Al-MCM-41-[Fe(bipy)Cl_4][bipy.H] by using KIO_4 as the oxidant however, no epoxide was observed (Schem 3), and selectivity toward benzil was obtained as follows (Table 2):

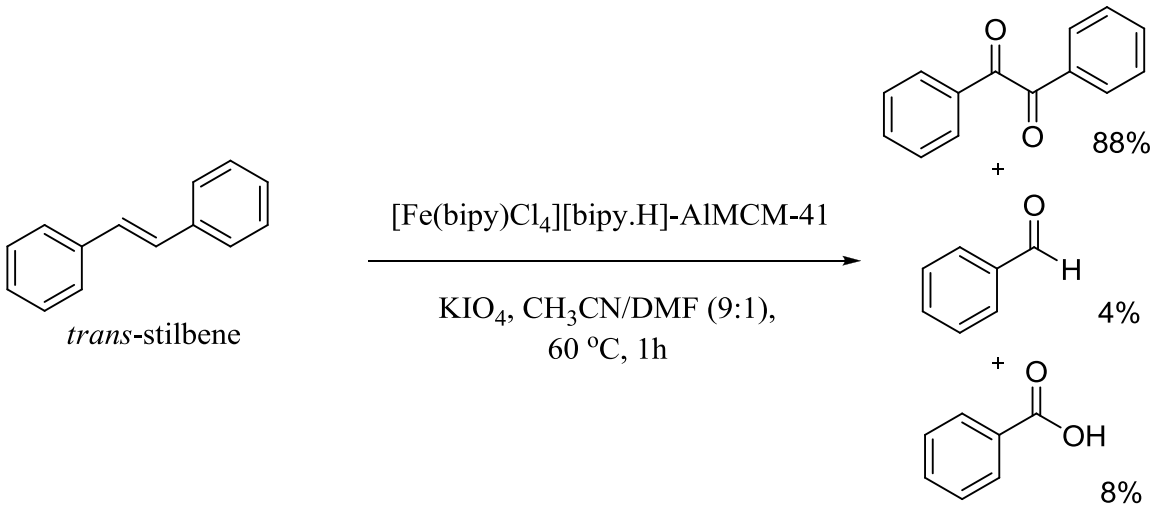

Scheme 3. Selectivity in the oxidation of *trans*-stilbene

The optimum catalyst loading was determined at room temperature in a 1:1 mixture of CH_3CN and DMF by using KIO_4 as the oxidant. This resulted in 64% selectivity toward benzil (Table 2, entry 3). At elevated temperature the ratio of the products was changed and the best selectivity toward benzil was obtained at 60 ^oC. Finally it was found that increasing the CH_3CN/DMF ratio to 9:1 results in excellent selectivity of 88%. A comparison was also made between Al-MCM-41-[Fe(bipy)Cl_4][bipy.H], Al-MCM-41, [Fe(bipy)Cl_4][bipy.H] and Al-MCM-41 mixed with [Fe(bipy)Cl_4][bipy.H] under optimized conditions (entries 7-10). It was found that Al-MCM-41-[Fe(bipy)Cl_4][bipy.H] has superiority in terms of recyclability and selectivity toward benzil. [Fe(bipy)Cl_4][bipy.H], on the other hand, resulted in lower reaction time and lower selectivity, and in the case of Al-MCM-41 mixed with [Fe(bipy)Cl_4][bipy.H] with exactly the same metal to host ratio (1.8% w/w Fe), lower selectivity and difficulty of catalyst recovery were major drawbacks.

Table 2. The effect of various parameters on the oxidation reaction of *Trans*-stilbene

Entry [a]	Catalyst	Catalyst loading (mg)	Temperature (^oC)	Yield [b] (%)		
				Bnezaldehyde	Benzil	Benzoic acid
1	Al-MCM-41-[Fe(bipy)Cl_4][bipy.H]	10	25	31	49 [c]	16
2	Al-MCM-41-[Fe(bipy)Cl_4][bipy.H]	20	25	26	59 [c]	12
3	Al-MCM-41-[Fe(bipy)Cl_4][bipy.H]	30	25	24	64 [c]	11
4	Al-MCM-41-[Fe(bipy)Cl_4][bipy.H]	35	25	20	63 [c]	11
5	Al-MCM-41-[Fe(bipy)Cl_4][bipy.H]	30	60	11	68 [c]	19
6	Al-MCM-41-[Fe(bipy)Cl_4][bipy.H]	30	90	5	60 [c]	34
7	Al-MCM-41-[Fe(bipy)Cl_4][bipy.H]	30	60	4	88 [d]	8
8	Al-MCM-41	30	60	8	6 [d]	3
9	[Fe(bipy)Cl_4][bipy.H]	10	60	31	40 [d, e]	28
10	Al-MCM-41 + [Fe(bipy)Cl_4][bipy.H]	30	60	33	39 [d]	27

[a] All reactions were carried out according to general experimental procedure.

[b] Isolated yields.

[c] CH_3CN/DMF= 1:1

[d] CH_3CN/DMF= 9:1

[e] 30 min reaction time

One of the main aims of the study was to evaluate reusability of the catalyst. To do so, the oxidation reaction of dibenzo[*b*,*f*][1,4]oxazepine to dibenzo[*b*,*f*][1,4]oxazepin-11(10*H*)-one was carried out in presence of the recycled catalyst in successive runs. From reaction run 1 to 5, the yields were 98%, 95%, 91%, 89% and 81%, respectively. Therefore after five runs, 17% decrease in the efficiency of the catalyst was observed. This result shows that Al-MCM-41-[Fe(bipy)Cl_4][bipy.H] can be utilized as a moderate and recyclable catalyst for the oxidative transformation of dibenzo[*b*,*f*][1,4]oxazepine to dibenzo[*b*,*f*][1,4]oxazepin-11(10*H*)-one. In order to confirm heterogeneity of the catalyst, the iron content of the catalyst was determined for the recycled catalyst of the 5^{th} run and a similar result (1.81%) was obtained, which confirmed that no considerable leaching was occurred during the course of reaction. To further approve this assumption, the oxidation reaction of dibenzo[*b*,*f*][1,4]oxazepine was interrupted halfway (30 min) and the catalyst was removed by filtration. The reaction was then continued for the rest of time (up to 60 min). At the end of this period only 65% of the product was obtained, which may further approve the success of encapsulation.

4. Conclusion

In conclusion, we have successfully incorporated the complex [Fe(bipy)Cl_4][bipy.H] into the channels of mesoporous Al-MCM-41 with no considerable change in the properties of the host. The whole assembly was used as an array of nanoreactors for selective oxidation of dibenzo[*b*,*f*][1,4]oxazepine and *trans*-stilbene. Further investigation in this context is currently under way in our laboratory.

Acknowledgments

Partial support of this study by the research council of university of Guilan is gratefully acknowledged. A. Khorshidi is grateful to Dr. S. Sohrabnejad for her generous support.

References

[1] I. Kuźniarska-Biernacka, A. M. Fonseca, I. C. Neves, *Inorg. Chim. Acta* 2013, **394**, 591.

[2] K. J. Balkus Jr, A. G. Gabrielov, *J. Inclusion Phenom. Mol. Recognit. Chem.* 1995, **21**, 159.

[3] K. O. Xavier, J. Chacko, K. K. Mohammed Yusuff, *J. Mol. Catal. A: Chem*. 2002, **178**, 275.

[4] S. Yamaguchi, T. Fukura, K. Takiguchi, C. Fujita, M. Nishibori, Y. Teraoka, H. Yahiro, *Catal. Today*, 2015, **242**, 261.

[5] C. Huber, K. Moller, T. Bein, *J. Chem. Soc. Chem. Commun.* 1994, 2619.

[6] H. Hamdan, V. Navijanti, H. Nur, M. Nazlan, M. Muhid, *Solid State Sci.*, 2005, **7**, 239.

[7] C. N. Rohitha, S. J. Kulkarni, N. Narender, *Synth. Commun.* 2013, **43**, 2853.

[8] M. Silva, M. J. F. Calvete, N. P. F. Goncalves, H. D. Borrows, M. Sarakha, A. Fernandes, M. F. Ribeiro, M. E. Azenha, M. M. Pereira, *J. Hazard. Mater.* 2012, **233-234**, 79.

[9] R. Ganesan, B. Viswanathan, *J. Mol. Catal. A: Chem*. 2002, **181**, 99.

[10] M. Alvaro, V. Forne´s, S. Garcia, H. Garcia, J. C. Scaiano, *J. Phys. Chem. B* 1998, **102**, 8744.

[11] Y. Umemura, Y. Minai, N. Koga, T. Tominaga, *J. Chem. Soc. Chem. Commun.* 1994, 893.

[12] S. Ray, S. Vaudevan, *Inorg. Chem*. 2003, **42**, 1711.

[13] S. K. Tiwary, S. Vasudevan, *Inorg. Chem.* 1998, 37, 5239.

[14] R. Higginbo, H. Suschitzky, *J. Chem. Soc.* 1962, 2367.

[15] A. Khorshidi, K. Tabatabaeian, *J. Mol. Catal. A: Chem*. 2011, **344**, 128.

[16] M. A. Zanjanchi, K. Tabatabaeian, A. Khorshidi, *Russ. J. Coord. Chem.* 2003, **29**, 686.

[17] V. Amani, N. Safari, H. R. Khavasi, P. Mirzaei, *Polyhedron* 2007, **26**, 4908.

[18] J. M. Kim, J. H. Kwak, S. Jun, R. Ryoo, *J. Phys. Chem*. 1995, **99**, 16742.

[19] V. Ahmadi, N. Safari, H. R. Khavasi, *Polyhedron* 2007, **26**, 4257.

[20] J. M. Kim, J. H. Kwak, S. Jun, R. Ryoo, *J. Phys. Chem.* 1995, **99**, 16742.

[21] K. Nagarajan, J. David, R. S. Grewal, T. R. Govindachari, *Indian J. Exp. Biol.* 1974, **12**, 217.

[22] K. Nagarajan, J. David, Y. S. Kulkarni, S. B. Hendi, S. J. Shenoy, P. Upadhyaya, *Eur. J. Med. Chem.* 1986, **21**, 21.

[23] J. M. Harrison, K. Brewster, T. D. Inch, *J. Labelled Comp. Radiopharm.* 1978, **14**, 375.

[24] E. Halamek, Z. Kobliha, *Talanta* 1993, **40**, 1189.

[25] I. W. Lawston, J. M. Harrison, T. D. Inch, D. B. Cooper, *J. Chem. Soc. Perkin Trans* 1979, **1**, 2642.

[26] K. Brewster, R. A. Chittenden, J. M. Harrison, T. D. Inch, C. Brown, *J. Chem. Soc. Perkin Trans* 1976, **1**, 1291.

[27] J. M. Harrison, R. J. Clarke, T. D. Inch, D. G. Upshall, *Experientia* 1978, **34**, 698.

[28] J. Schmutz, F. Kunzle, F. Hunziker, R. Gauch, *Helv. Chim. Acta* 1967, **50**, 245.

[29] C. F. Howell, R. A. Hardy, N. Q. Quinones, *Patent No. 3,444,169*, **1969**.